Mol Neurobiol (2012) 45:17–29
DOI 10.1007/s12035-011-8215-z

An Aberrant Cerebellar Development in Mice Lacking Matrix Metalloproteinase-3

Inge Van Hove · Mieke Verslegers · Tom Buyens · Nathalie Delorme · Kim Lemmens · Stijn Stroobants · Ilse Gantois · Rudi D'Hooge · Lieve Moons

Received: 3 October 2011 / Accepted: 24 October 2011 / Published online: 23 November 2011

Abstract Cell–cell and cell–matrix interactions are necessary for neuronal patterning and brain wiring during development. Matrix metalloproteinases (MMPs) are proteolytic enzymes capable of remodelling the pericellular environment and regulating signaling pathways through cleavage of a large degradome. MMPs have been suggested to affect cerebellar development, but the specific role of different MMPs in cerebellar morphogenesis remains unclear. Here, we report a role for MMP-3 in the histogenesis of the mouse cerebellar cortex. MMP-3 expression peaks during the second week of postnatal cerebellar development and is most prominently observed in Purkinje cells (PCs). In MMP-3 deficient (MMP-3$^{-/-}$) mice, a protracted granule cell (GC) tangential migration and a delayed GC radial migration results in a thicker and persistent external granular layer, a retarded arrival of GCs in the inner granular layer, and a delayed GABAergic interneuron migration. Importantly, these neuronal migration anomalies, as well as the consequent disturbed synaptogenesis on PCs, seem to be caused by an abnormal PC dendritogenesis, which results in reduced PC dendritic trees in the adult cerebellum. Of note, these developmental and adult cerebellar defects might contribute to the aberrant motor phenotype observed in MMP-3$^{-/-}$ mice and suggest an involvement of MMP-3 in mouse cerebellar development.

Keywords Matrix metalloproteinase-3 · Development · Cerebellum · Neuronal patterning · Purkinje cell dendritogenesis · Neuronal wiring

I. Van Hove · M. Verslegers · T. Buyens · N. Delorme · K. Lemmens · L. Moons (✉)
Laboratory of Neural Circuit Development and Regeneration, Animal Physiology and Neurobiology Section, Department of Biology, K.U.Leuven, Naamsestraat 61, Box 2464, 3000 Leuven, Belgium
e-mail: lieve.moons@bio.kuleuven.be

S. Stroobants · I. Gantois · R. D'Hooge
Laboratory of Biological Psychology, Department of Psychology, K.U.Leuven, Tiensestraat 102, 3000 Leuven, Belgium

Introduction

The cerebellum is a good model system to study developmental brain processes because of its limited number of cell types, its well characterized wiring pattern, and its largely postnatal development. Granule cell precursors (GCPs) proliferate massively in the embryonic and postnatal stage to form the external granular layer (EGL), thereby generating the most abundant cell type of the cerebellum. During the first postnatal week, postmitotic granule cells (GCs) start to migrate tangentially in the deeper EGL and radially along Bergmann glia fibers in the molecular layer (ML) towards their final position in the internal granular layer (IGL) [1]. Concomitant with dynamic Purkinje cell (PC) dendritic outgrowth, parallel fibers of differentiated GCs are massively contacting the distal parts of the dendritic trees [2]. These excitatory synaptic contacts on PC dendrites are formed before the inhibitory synapses, made up by GABAergic interneurons (INs). These INs consist of Golgi cells, present in the IGL and innervating the GCs, and basket and stellate cells, residing in the ML and intensively contacting the PCs during the second and third postnatal week [3]. The intercellular interactions taking place during cerebellar development, e.g., GCs influencing PC dendritogenesis and vice versa, PCs affecting GC survival, proliferation, and migration, are necessary to built up a proper and functional cerebellar circuitry [2].

MMP-3 (stromelysin-1; EC 3.4.24.17) belongs to the matrix metalloproteinase (MMP) family, proteinases cleaving structural elements of the extracellular matrix and many molecules involved in signal transduction. Besides a proven detrimental role in neurological diseases, a beneficial role for MMPs in key physiological and regenerative brain events is emerging. Previous studies already demonstrated an involvement of MMP-3 in axon guidance, dendrite extension, neuronal apoptosis, synaptogenesis, and plasticity [4]. Based on its expression pattern, MMP-3 was suggested to be involved in GC migration and axonal growth in the rat cerebellum [5]. Among the other MMPs, MMP-2, MMP-9, and MT5-MMP are known to be expressed in the developing cerebellum [5]. However, until now, only a role for MMP-9 in cerebellar morphogenesis was established by functional studies in which MMP-9 activity was blocked by specific inhibitors and function-blocking antibodies and in MMP-9 knockout mice [6, 7].

To address whether MMP-3 plays a role in the development of the mouse cerebellar cortex, both in vivo, ex vivo, and behavioral studies were performed in MMP-3-deficient mice.

Materials and Methods

Animals

All experiments were performed in MMP-3-deficient (MMP-3$^{-/-}$) and wild-type (WT) mice from a similar background (50% Bl6×25% B10×25% RIII) (Mudgett, Merck labs). For most parts of the study, littermates were used. Genotyping was performed on tail DNA with a forward primer (5′ AACATGGAGACTTTGTCCCTT 3′) and a reverse primer (5′ CAGTGACATCCTCTGTCCAT 3′) for the WT mice and a forward primer (5′ GAGGAGCCA GAGAACCTACTGAAG 3′) and a reverse primer (5′ TCATAGCCTGAAGAACGAGATCAGC 3′) for the mutant mice. All animal experiments were approved by the Institutional Ethical Committee of the K.U.Leuven and in strict accordance with the European Communities Council Directive of 24 November 1986 (86/609/EEC).

Real-Time PCR

Mice (between P0 (postnatal day 0, day of birth) and P70) were anesthetized with sodium pentobarbital (35 mg/kg, Ceva) and decapitated. Cerebella were collected, immediately frozen in liquid nitrogen, and total RNA was isolated using TRI-Reagent (Applied Biosystems). Subsequently, cDNA was synthesized with the Quantitect Reverse Transcription kit (Qiagen), and real-time PCR reactions were performed using the SYBR® Green method (Invitrogen) with previously described primers for MMP-3 and 18S rRNA [8, 9]. Relative gene expression was calculated using the gene expression CT difference (GED) formula [10] and represented as fold difference towards levels at P6.

Histology, Immunohistochemistry and In Situ Zymography

For all histological and immunohistochemical stainings, mice of various developmental stages were deeply anesthetized and intracardially perfused with 4% paraformaldehyde (PFA). Sagittal 10 μm-thick cryostat sections were cut. General morphology was studied using hematoxylin–eosin (H&E) stainings. Immunostaining for MMP-3 was performed with a primary rabbit antibody against MMP-3 (Santa Cruz, sc-6839-R, used at 1/50), followed by incubation with a horseradish peroxidase (HRP)-labeled goat anti-rabbit secondary antibody (Dako). Amplification via the TSA^{TM} Biotin system (Perkin Elmer) was followed by an HRP-labeled streptavidin and subsequent staining using DAB as chromogen. Phenotypical fluorescent stainings were performed on similar sections, using appropriate Alexa Fluor secondary antibodies (Invitrogen) or the TSA™ FT/Cy3 System (Perkin Elmer) with the following primary antibodies: anti-GFAP (Dako, Z0334, used at 1/1000), anti-Calbindin D-28K (Sigma-Aldrich, C9848, 1/1000), anti-p27 (Santa Cruz, sc-1641, 1/50), anti-VGLUT2 (Invitrogen, 42–7800, 1/250), anti-VGLUT1 (Synaptic Systems, 135 302, 1/1000), anti-Pax-6 (Covance, PRB-278P, 1/300), anti-Pax-2 (Invitrogen, 71–6000, 1/750), anti-BrdU (AbD serotec, OBT0030CX, 1/300), anti-Phospho-Histone H3 (Cell Signaling, 9701, 1/1000), anti-TAG-1 (Developmental Studies Hybridoma Bank, 1/50), anti-VGAT (Synaptic Systems, 131 002, 1/200), anti-Active Caspase-3 (Gentaur, 3015–100, 1/20). Apoptosis was also detected using TUNEL (in situ cell death detection kit, Roche Applied Science) labeling.

In situ zymography was performed immediately after cryo-sectioning on 30 μm unfixed brain slices from different postnatal ages. Controls implied pre-incubation of sections at room temperature for 1 h with EDTA (20 mM in DMSO) or a more specific MMP-3 inhibitor (5 μM in milli-Q) (MMP-3 inhibitor I, Calbiochem). Subsequently, all sections were incubated overnight with 100 μg/ml FITC-casein in zymogram buffer (Invitrogen) at 37°C in a dark, moist environment, rinsed with PBS, and fixed during 20 min with PFA.

All bright-field or fluorescently labeled sections were examined under a Zeiss Imager Z1 microscope, and histomorphometric analyses were performed using the digital image processing software Axiovision (Zeiss). All cell counts and area measurements were performed on similar areas of comparable midsagittal sections over a distance of 400 μm within cerebellar lobe IX. To measure

the relative VGLUT1 and VGLUT2 positive areas, the surface of the ML and the corresponding VGLUT1$^+$ and VGLUT2$^+$ area in that surface was determined over a distance of 400 μm in lobe IX of comparable midsagittal sections. Caspase-3$^+$ cell numbers were determined in all vermal lobes and VGAT$^+$ synaptic contacts were counted per Purkinje cell along lobe IX.

BrdU Birthdating Experiments

For analysis of GC proliferation, WT and MMP-3$^{-/-}$ mice were injected intraperitoneally with 5-bromodeoxyuridine (BrdU, 100 mg/kg body weight) at P0, P3, P6, P8, P10, P12, and P15 and perfused with 4% PFA 3 h later. Mice used for studying the GC migration profile were given a BrdU injection at P6 and P10 and were sacrificed 2, 5, or 11 days later, respectively, at P8, P12, P15, and P21.

Single or combined immunostainings were performed as described above, and the number of BrdU$^+$ cells per layer was determined over a pial distance of 400 μm in lobe IX of midsagittal sections.

Golgi–Cox Staining

For visualization of PC dendrites, P12 and 3 months old WT and MMP-3$^{-/-}$ mice were anesthetized and perfused with 0.9% NaCl. Cerebella were dissected and cut into two halves at the midsagittal line, rinsed with milli-Q water, and stained according to the manufacturer's instructions (FD rapid Golgi stain kit, FD Neurotechnologies). The brain halves were embedded in 20% gelatine, vibratome-sectioned at 70 μm thickness, and mounted on slides. The PC primary dendrite length and dendritic tree size were measured on bright-field images, taken with a Zeiss Imager Z1 microscope and Axiovision software, on at least 65 individual PCs of entire cerebellar sections, from three mice per genotype and per age.

Cerebellar Microexplant Cultures

P8 WT and MMP-3$^{-/-}$ mice were decapitated and the cerebellar cortices were quickly dissected in Gey's balanced salt solution, containing 0.65% glucose. Meninges were removed and the vermis was selected and cut into 200 μm sagittal slices using a McIlwain Tissue Chopper. Mainly, EGL was dissected, cut into 200 μm pieces, and subsequently plated on poly L-lysin/laminin coated coverslips in 50% basal medium eagle, 25% Hank's balanced salt solution, 25% inactivated horse serum+penicillin/streptomycin and 4 mg/ml methylcellulose. After 48 h, microexplants were fixed overnight with 4% PFA and stained for β-III tubulin (Sigma-Aldrich, T8660). The length of the six longest parallel fibers and the number of GCs that migrated over 50 μm from the core explant were analyzed in explants with homogeneous radial process outgrowth, relative to the explant perimeter (see also Fig. 3e).

Western Blotting

Cerebella of P8 mice were dissected and homogenized in lysis buffer (50 mM Tris–HCl, pH 8, 300 mM NaCl, 0.5% NP-40, 0.5% sodium deoxycholate, 1 mM EDTA, pH 8 and 0.1% SDS), supplemented with protease inhibitors. Homogenates (10 μg) were loaded on 4–12% SDS-PAGE and transferred onto a polyvinylidine fluoride membrane. Overnight incubation with primary antibodies to BDNF (Santa Cruz, sc-546, 1/100) or GAPDH (Millipore, MAB374, 1/20000) was followed by a 1-h incubation with HRP-labeled secondary antibodies (Dako, 1/2000). Protein bands were visualized using a luminol-based enhanced chemiluminescent kit (Thermo Scientific).

Motor Performance Tests

Treadmill analyses were used to define gait parameters (base distance and overlap distance) in P16 male and female WT and MMP-3$^{-/-}$ mice. Three training trials were conducted at a speed of 19 cm/s and at a 5° slope. Afterwards, mice were forced to run on the treadmill with a speed of 16 cm/s and a slope of 0° during a 60 s test trial. Video-recording and subsequent footprint data analysis with Matlab enabled the determination of several gait parameters.

Next, adult mice (8 to 9 weeks) of both sexes were tested for circadian activity, rotarod, and balance beam performance. Circadian cage activity was measured by placing the animals individually into 26.7×20.7 cm transparent cages between three IR beams for 23 h in a normal day–night rhythm. The total number of photobeam-crossings was automatically counted every 30 min [11]. General motor behavior and equilibrium was first tested using an accelerating rotarod (MED Associates, St. Albans, Vermont, USA). After a training phase of 2 min at 4 rpm, mice were forced to run on the accelerating rotarod, starting from 4 until 40 rpm in 5 min. This test was performed three times a day over three sequential days and latency to fall was recorded. Secondly, mice were subjected to the balance beam test. Three days of testing on the largest wooden square beam were followed by 1 day of trials on square and round beams with decreasing diameter (28, 12, 9, and 5 mm for the square beams and 28, 17, 11, and 5 mm for the round beams). All mice were forced to traverse each of the beams twice and the number of paw faults or slips was noted by two observers, blinded for the genotype.

In addition, male and female postnatal and adult mice were subjected to a hindlimb extension test as previously described [12].

Statistical Analyses

All values are represented as mean±SEM. Statistical analysis for histomorphometric measurements and gait analysis was performed using a Student's *t* test. For cage activity, balance beam and rotarod tests, a repeated-measures 2-way ANOVA and Student's *t* test was used. Multilevel analysis (SAS Proc Mixed) was applied for explant and PC data analysis. For all statistical tests, a *p* value of 0.05 was considered statistically significant.

Results

Spatiotemporal Expression of MMP-3 mRNA and Protein in the Developing Cerebellum

RT-PCR analysis revealed increasing MMP-3 mRNA levels during cerebellar development with maximal expression around P15 and a steep decline towards the end of the third postnatal week (Fig. 1a). Immunostainings showed MMP-3 protein expression at P0 in the cell soma of the prospective white matter (WM) and the future Purkinje cell layer (PCL) (Fig. 1b). At P6, MMP-3 protein was visible in the cells and neuropil of the PCL and weakly expressed in cells of the EGL and IGL (Fig. 1b). From P10 on, also all Golgi cells, identified by their location and morphology, showed intense MMP-3 immunoreactivity. At this stage, the PCs and their proximal dendrites, the Golgi cell somata in the IGL and cells in the WM were the major producers of MMP-3 (Fig. 1b). From P12 on and at least until P21, the MMP-3 expression pattern remained similar to the one observed at P10, but also interneurons (INs) in the ML, located near the PCL and therefore presumably basket cells (BCs), and randomly spread cell somata from GCs or INs in the IGL weakly expressed MMP-3 protein. In situ zymography visualized active MMP-3 on cerebellar sections of WT animals (Fig. 1c). Sections incubated with MMP-3 inhibitor I (Calbiochem) showed a generally reduced fluorescence level (Fig. 1c). In addition, the fluorescent signal was also abolished upon preincubation with buffer or EDTA, a non-specific metalloproteinase inhibitor (not shown). At all stages of cerebellar development, MMP-3 activity could be detected in the PC somata, Golgi cells, and to a lesser extent in cells of the EGL and IGL, INs of the

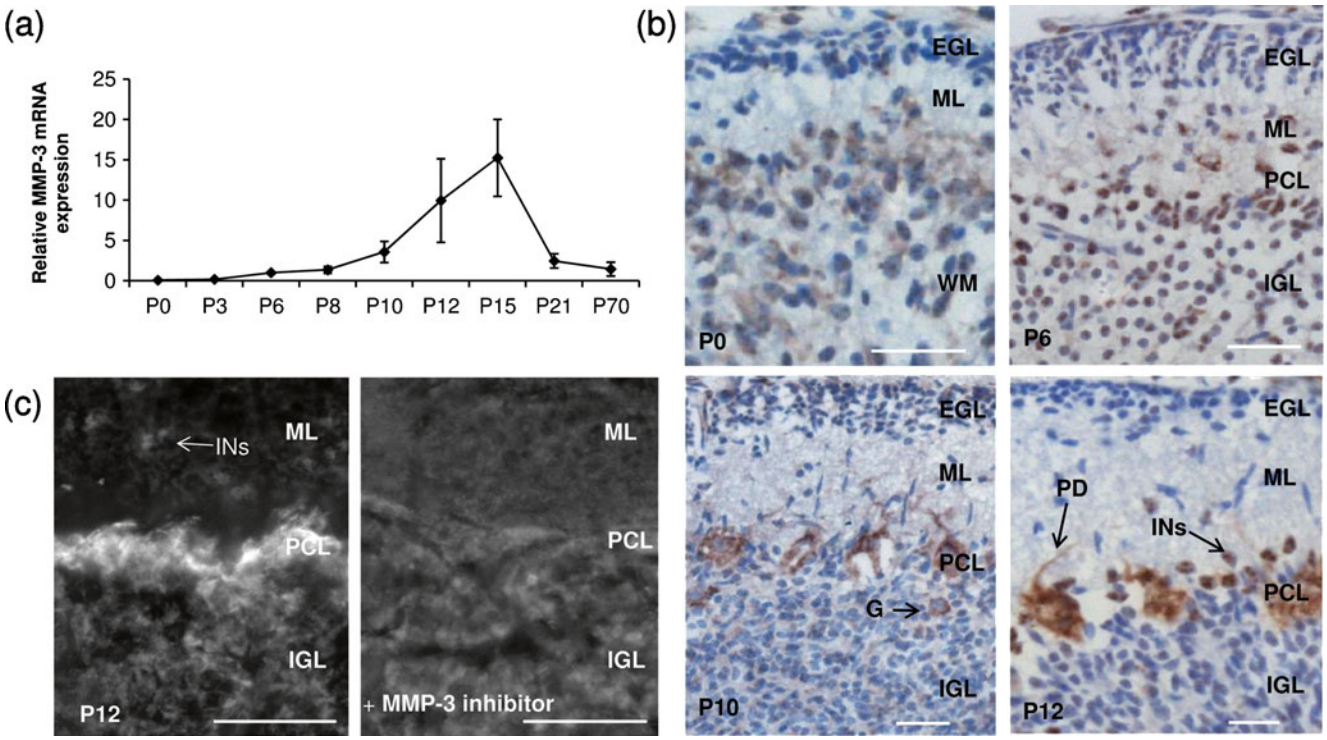

Fig. 1 MMP-3 expression and activity in the developing cerebellum. **a** MMP-3 mRNA levels increase during development and peak at the end of the second postnatal week. Data (mean±SEM) are normalized to 18S rRNA levels and relative to levels at P6. **b** Immunostaining for MMP-3 reveals, throughout development, an increasing protein expression in PC somata and primary dendrites (PD), Golgi cells (G), and ML interneurons (INs). Weak staining is also visible in EGL and IGL cells. **c** In situ zymography shows high MMP-3 activity in the PCL and lower fluorescent staining in the ML interneurons and IGL. The fluorescent signal is strongly reduced after preincubation with a specific MMP-3 inhibitor. Scale bars in panels **b** and **c**, respectively, 50 and 75 μm

ML and WM cells. Overall, MMP-3 expression levels and activity remarkably increase during cerebellar development and peaked during the second postnatal week, coinciding with extensive PC tree branching and ongoing GC migration [2].

MMP-3 Deficiency Results in an Increased EGL Thickness

Hematoxylin and eosin-stained mid-sagittal sections did not show obvious phenotypic abnormalities in the overall cytoarchitecture of cerebella of MMP-3$^{-/-}$ mice, as compared to WT animals; however, a more detailed morphometric analysis revealed an increased EGL thickness in MMP-3$^{-/-}$ cerebella from P8 on. It is well known that towards the end of the first postnatal week, GC precursor (GCP) proliferation declines [13] (see also Fig. 2c) and GCs start to migrate. As a result, between P6 and P8, the EGL thickness of WT pups decreased by 20.0±2.0%, while this was only by 3.4±3.1% in MMP-3$^{-/-}$ pups (Fig. 2a). Furthermore, at P15, the EGL of WT mice had almost disappeared, while MMP-3$^{-/-}$ cerebella still showed an apparent EGL. Interestingly, the increased EGL area was due to a higher GC number, not to a difference in cell size or in matrix between the GCs (Fig. 2b). Overall, MMP-3$^{-/-}$ mice show an increased GC number and consequently a thicker EGL from P8 on.

MMP-3 Deficiency Influences GC Proliferation but only at a Later Stage During Development

To further investigate whether the observed increase in EGL thickness and GC number is due to differences in GCP proliferation rate, 3 h BrdU pulse studies were performed at various postnatal ages. Of note, in WT as well as in MMP-3$^{-/-}$ mice, the GCP proliferation rate was already found to decrease after P3 (Fig. 2c). Although proliferation seems to be slightly increased at all developmental stages studied, we did not detect significant differences in the GCP proliferation rate between mutant and control mice from P0 until P10 or at P15 (Fig. 2c). Remarkably, at P12, when the GCP proliferation rate in WT animals is abruptly decreasing, a clear difference in proliferation was noticed in MMP-3$^{-/-}$ mice. Immunostainings for the mitosis marker "Phospho-Histone H3 (PH3)" again revealed no differences in the number of PH3^{+} cells in the EGL of mutant and WT mice until P10 (data not shown), but significantly more PH3^{+} cells were counted in the EGL of MMP-3$^{-/-}$ cerebella at P12 (Fig. 2d). Our data thus indicate that proliferation deficits do not account for the increased EGL thickness in the MMP-3$^{-/-}$ cerebella at P8 and P10 but might contribute to

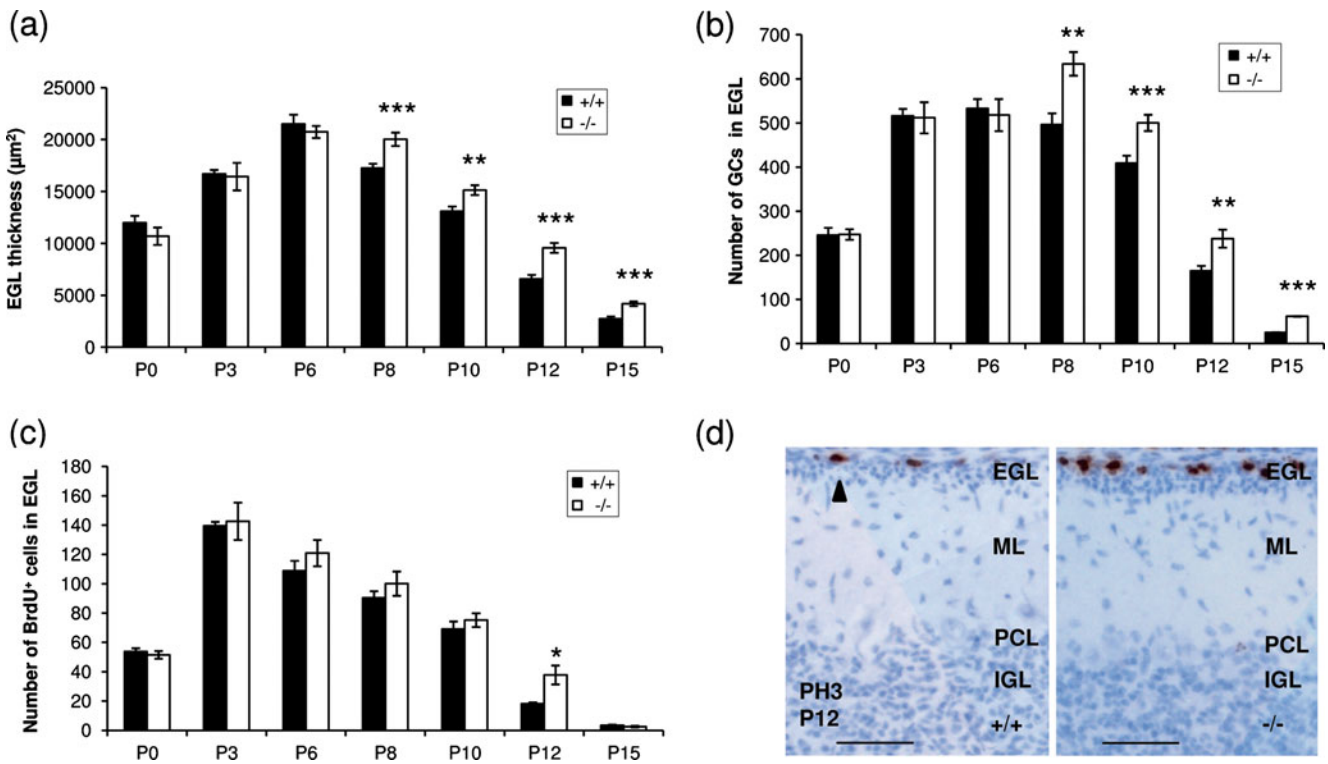

Fig. 2 Increased EGL thickness in MMP-3$^{-/-}$ cerebella. **a**, **b** Morphometric analyses on sagittal H and E-stained sections show, from P8 on, a decrease in EGL thickness (**a**) and in the number of GCs (**b**) in WT cerebella, while both remain significantly elevated in MMP-3$^{-/-}$ cerebella. **c** Using 3 h BrdU pulse experiments, the number of proliferating GCPs is found to be significantly increased in MMP-3$^{-/-}$ cerebella only at P12. **d** Immunostainings for PH3 (*arrowhead*) confirm the increased GCP proliferation rate in MMP-3$^{-/-}$ mice at P12. *Scale bar*, 50 µm. All the area measurements and cell countings are performed on similar midsagittal cerebellar sections over a pial distance of 400 µm in lobe IX. Data are represented as mean±SEM (*p<0.05, **p<0.01, or ***p<0.005)

the difference in EGL thickness at P12 and consequently at P15.

MMP-3 Deficiency does not Affect GC Apoptosis in the EGL

To verify whether the increased amount of GCs in the EGL of MMP-3$^{-/-}$ mice might be attributable to a decrease in GC apoptosis and to check for possible (secondary) apoptotic deficits later on during development, caspase-3 and TUNEL stainings were performed. At P8, P10, and P12, the number of apoptotic cells in the EGL, analyzed in whole cerebellar vermal sections, was equal in both genotypes (data not shown). Therefore, the increased EGL thickness is not attributable to aberrant apoptotic processes.

MMP-3 Deficiency Affects the Thickness of the Deep EGL

To determine whether the observed increase in EGL thickness is due to changes in the superficial or deeper EGL, immunostainings for TAG-1, a cell adhesion molecule transiently expressed on GC axons (parallel fibers) [14], and for p27, a cyclin-dependent kinase inhibitor expressed by GCs after cell cycle exit [15] were performed. The superficial EGL zone, where GCPs actively proliferate, resembles the TAG-1$^-$ or p27$^-$ area, while the deeper EGL zone, where differentiated postmitotic GCs extend their parallel fibers and migrate tangentially, is defined as the TAG-1$^+$ or p27$^+$ area. At P8 and P10, the TAG-1$^+$ area was significantly larger in MMP-3$^{-/-}$ mice as compared to WT animals, while the TAG-1$^-$ area was similar in size (Fig. 3a). Remarkably, at P12, also the TAG-1$^-$ area was significantly enlarged in mutant mice. Analyses on p27-stained sections confirmed these findings (data not shown). These data correlate with the previously observed higher GCP proliferation rate in MMP-3$^{-/-}$ animals at P12 (Fig. 2c). Taken together, the thicker EGL in MMP-3$^{-/-}$ mice at later postnatal stages can be caused in part by a sustained high GCP proliferation rate, but this cannot account for the increased thickness of the deep EGL observed at earlier developmental stages.

MMP-3 Deficiency Delays Radial GC Migration

To further investigate a possible perturbed GC migration, BrdU birthdating experiments were performed. At first, the ratio of BrdU$^+$ cells per layer over the total number of BrdU$^+$ cells was analyzed at P8 (after injection at P6), which resulted in a significantly higher percentage of BrdU$^+$ GCs in the EGL and a significantly lower percentage in the IGL of MMP-3$^{-/-}$ mice (Fig. 3b), indicating anomalies in GC distribution. No differences were found in the percentage of cells in the ML nor in the total number of BrdU$^+$ cell counts in all layers (336±17 BrdU$^+$ cells in WT vs. 338±9 in MMP-3$^{-/-}$ pups, n=6–5, p=NS). The latter findings indicate that no GC proliferation, but rather radial GC migration abnormalities in the EGL, are underlying the higher EGL thickness observed in MMP-3$^{-/-}$ cerebella at P8.

At P12, 2 days after BrdU injection at the peak of migration (P10), a similar pattern, namely a significantly higher percentage of BrdU$^+$ GCs in the EGL and a lower percentage in the IGL was observed in MMP-3$^{-/-}$ cerebella as compared to WT brains (Fig. 3c). Despite a similar amount of BrdU$^+$ cells in the IGL, a significantly higher number of BrdU$^+$ cells was located in the EGL and ML of MMP-3$^{-/-}$ cerebella (data not shown). Consequently, the total number of BrdU$^+$ cells was significantly higher in MMP-3$^{-/-}$ cerebella (109±10 BrdU$^+$ cells in WT vs. 151±10 in MMP-3$^{-/-}$ pups, n=10, p<0.01). These findings again indicate a delayed radial GC migration towards the IGL and a higher GCP proliferation rate in the EGL of MMP-3$^{-/-}$ cerebella between P10 and P12.

Five days after BrdU injection (P15), the distribution of BrdU$^+$ GCs in the MMP-3$^{-/-}$ cerebella showed a similar trend but was no longer significantly different from that in WT brains (Fig. 3d). However, at P15, a significantly increased number of BrdU$^+$ cells was detected in each layer of the MMP-3$^{-/-}$ cerebella (total number of BrdU$^+$ cells, 72±8 BrdU$^+$ cells in WT vs. 103±8 in MMP-3$^{-/-}$ pups, n=10–9, p<0.005). Moreover, at P21, 11 days after injection, the number of BrdU$^+$ GCs was still slightly higher in the IGL of MMP-3$^{-/-}$ mice as compared to WT animals (number of BrdU$^+$ cells in the IGL, 51±5 BrdU$^+$ cells in WT vs. 71±7 in MMP-3$^{-/-}$ mice, n=5, p=NS), suggestive of an increased GCP proliferation around P12 and consequently a delayed radial GC migration.

Thus, MMP-3 seems necessary to allow differentiated GCs to exit the EGL as MMP-3 deficiency leads to an increased EGL thickness from P8 on. Importantly, this GC stalling in the deep EGL delays the time point at which GCs reach the IGL, which is supported by the significantly reduced IGL thickness in MMP-3$^{-/-}$ cerebella at P8 and P10 (IGL area at P8, 64,277±1,584 μm^2 in WT vs. 52,747±3,154 in MMP-3$^{-/-}$ cerebella (n=5, p<0.05); IGL area at P10, 64,085±2,487 in WT vs. 56,640±1,716 in MMP-3$^{-/-}$ cerebella (n=5, p<0.05)). Furthermore, this GC stalling affects the GCP proliferation rate in the superficial EGL, which finally results in a prolonged radial GC migration in MMP-3$^{-/-}$ cerebella.

MMP-3 Deficiency Increases GC Parallel Fiber Outgrowth and Tangential Migration

In order to explain the observed delayed radial GC migration in MMP-3$^{-/-}$ mice, we first looked for possible defects in parallel fiber outgrowth and tangential migration of GCs using microexplants of P8 cerebella (Fig. 3e). The length of

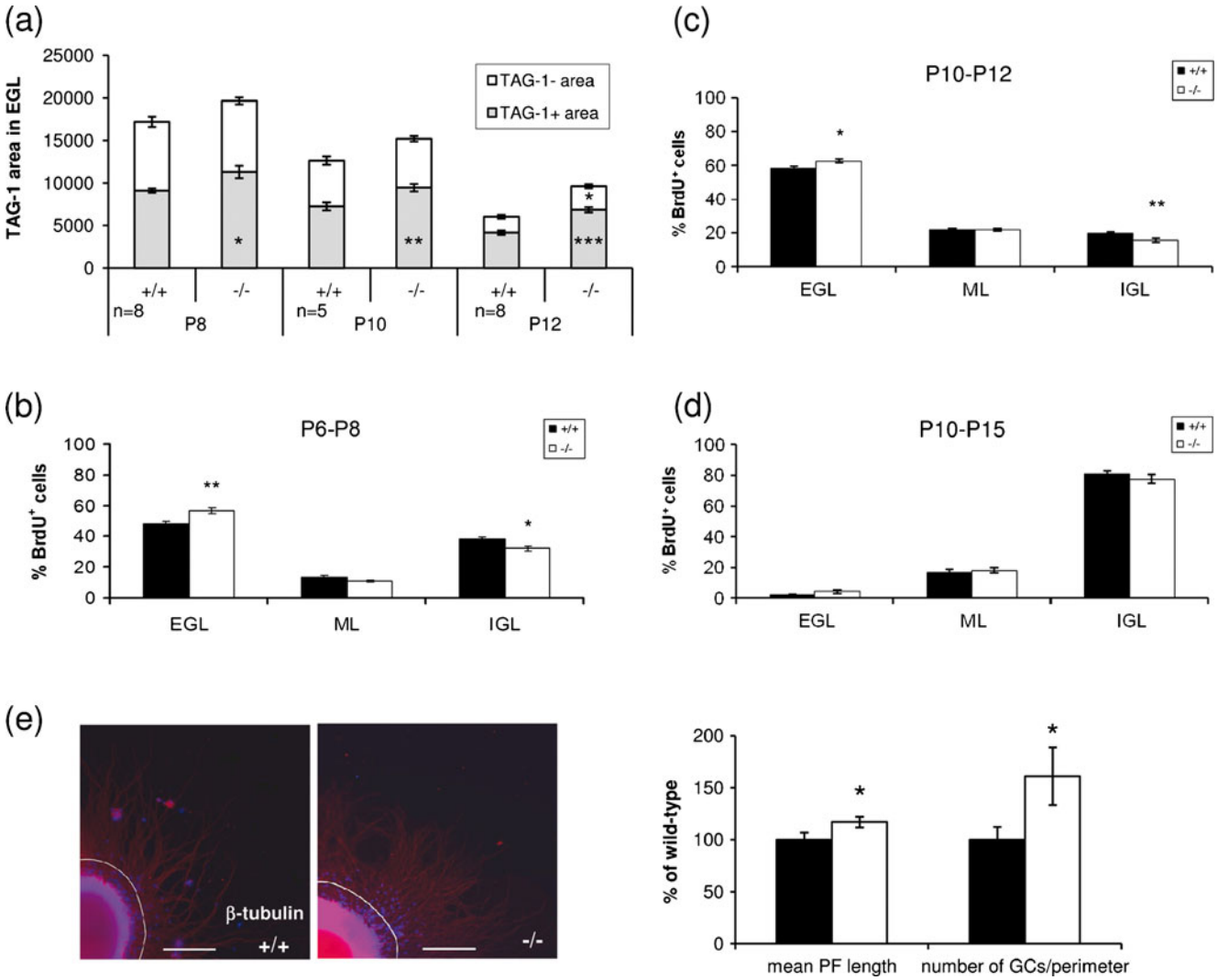

Fig. 3 Aberrant GC migration in MMP-3$^{-/-}$ cerebella. **a** Analysis of the proportion of the TAG-1^{-} area (white beam) to the TAG-1^{+} area (gray beam) in the EGL of MMP-3$^{-/-}$ and WT pups reveal an increased TAG-1^{+} area or inner EGL in MMP-3$^{-/-}$ cerebella at P8, P10, and P12. At P12, also the TAG-1^{-} area is significantly enlarged in the MMP-3$^{-/-}$ EGL. **b** BrdU birthdating experiments at P6 reveal a significantly higher percentage of labelled cells in the EGL and a reduced percentage in the IGL of P8 MMP-3$^{-/-}$ mice. **c**, **d** Injection of BrdU at P10 reveals a higher percentage of BrdU^{+} cells in the EGL and a lower percentage in the IGL of MMP-3$^{-/-}$ mice at P12 (**c**), but at P15, the distribution of BrdU^{+} cells is rather similar in both genotypes (**d**). All the morphological measurements (**a**–**d**) are performed on similar midsagittal cerebellar sections over a pial distance of 400 μm in lobe IX. **e** Representative microexplants from WT and MMP-3$^{-/-}$ cerebella with radially outgrowing parallel fibers (PFs) and migrating GCs. Analysis of the length of the PFs and the number of GCs that migrated over a distance of 50 μm or more from the core explant (=outside from the *red circle*) reveals a significantly increased outgrowth in MMP-3$^{-/-}$ mice. *Scale bar*, 200 μm. Data are represented as mean±SEM (*p<0.05, **p<0.01, or ***p<0.005)

the parallel fibers (PFs) extending from the transgenic explants was significantly increased as compared to the WT explants (Fig. 3e). As GCs migrate along previously formed parallel fibers during tangential migration [16], we also analyzed the number of migrating GC nuclei. Microexplants from mutant mice showed a significantly increased number of migrating GCs (Fig. 3e). Taken together, these ex vivo data indicate that both GC parallel fiber outgrowth and GC tangential migration are increased by MMP-3 deficiency. Although these ex vivo data might not entirely reflect the in vivo situation, they provide evidence for the observed increased size of the deep EGL. Together with the data obtained using immunostainings for TAG-1 and p27 and revealing an increased inner EGL thickness in P8 MMP-3$^{-/-}$ brains, these findings are suggestive for a delayed onset of radial GC migration in MMP-3$^{-/-}$ cerebella.

MMP-3 Deficiency does not Affect Bergmann Glia Fiber Morphology

As GCs accomplish their inward radial migration along Bergmann glia fibers, the morphology of these fibers was

examined. However, no abnormalities in the radial organization pattern or density of the GFAP-labeled Bergmann glia were found at any developmental time point analyzed (data not shown), suggesting that the observed radial migration problems are not attributable to any changes in the structure of these glial processes.

MMP-3 Deficiency Affects Purkinje Cell Dendrite Morphology

As MMP-3 is expressed by PC soma and primary dendrites, which are also known to influence GC proliferation and migration [17–20], a possibly altered PC morphology was determined on Calbindin-stained cerebella at different postnatal days. No differences could be found in the number, diameter, or alignment of PC somata in postnatal and adult WT and MMP-3$^{-/-}$ cerebella (data not shown). However, additional Golgi stainings, performed to distinguish separate PCs and their dendrites [21, 22] in P12 and adult mice, revealed a reduction in the length of the primary dendrites (PDs) by 17% (n=3, p<0.05) at P12 and by 26% (n=3, p=0.005) in adult MMP-3$^{-/-}$ cerebella (Fig. 4a). Furthermore, in the adult stage, the size of the dendritic trees was decreased by 10% in the absence of MMP-3 (n=3, p<0.01). Also at P12, a reduced dendritic tree size was observed in MMP-3$^{-/-}$ mice. Significance was not reached here (n=3, p=0.07), most likely because of the high variability in PC arborization at this developmental age (Fig. 4a) [23]. In conclusion, MMP-3$^{-/-}$ deficiency results in an abnormal dendritic growth of PCs, which might underlie the observed aberrant cerebellar development in these animals. Importantly, abnormal

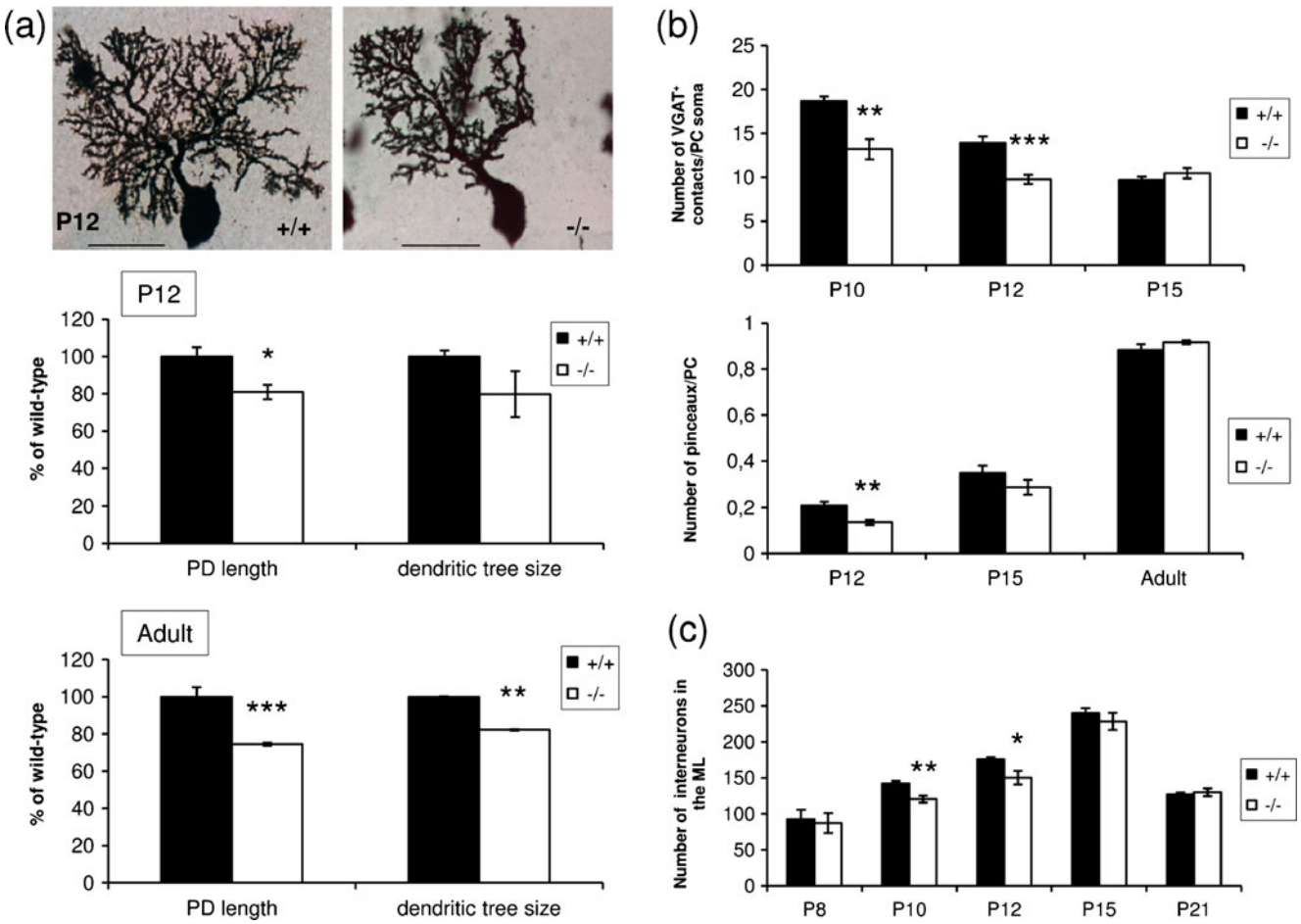

Fig. 4 Aberrant PC dendritic morphology and synaptogenesis in MMP-3$^{-/-}$ cerebella. **a** Representative pictures of P12 Golgi-stained PCs in WT and MMP-3$^{-/-}$ cerebellar sections. Morphometric analyses on entire sections show a decreased PC primary dendrite (PD) length and a reduced dendritic tree size in P12 and adult MMP-3$^{-/-}$ cerebella. Measurements were performed on at least 65 PCs per genotype and per age. **b** VGAT immunostainings reveal a reduced number of VGAT^{+} BC contacts on the PC soma in MMP-3$^{-/-}$ cerebella at P10 and P12, with a consequent transient delay in pinceau formation on the PC axon hillock. **c** Analysis of Pax-6 immunostainings show a significantly reduced number of interneurons in the ML at P10 and P12 in MMP-3$^{-/-}$ cerebella. VGAT and Pax-6 measurements were performed over a distance of 400 μm in lobe IX of comparable midsagittal sections. *Scale bar*, 50 μm. Data are represented as mean± SEM (*p<0.05, **p<0.01, or ***p<0.005)

PC dendritic trees are still present in adult MMP-3$^{-/-}$ brains.

MMP3 Deficiency Retards Synapse Maturation of GC Axons on PC Dendrites

To further study whether the delayed onset of GC radial migration and the abnormal PC dendritic development had any effect on GC-PC synapse maturation, immunostainings for the presynaptic vesicular glutamate transporter VGLUT2 were performed on cerebella of P12, P15, and P21 mice. During the first postnatal week, parallel fibers express VGLUT2. However, during the second and third postnatal week, VGLUT2 expression is replaced by VGLUT1, upwards across the ML, resulting in parallel fibers exclusively expressing VGLUT1 by the end of the fourth postnatal week [24]. Morphometrical analyses showed an increased relative VGLUT2^{+} area in the ML of MMP-3$^{-/-}$ mice (VGLUT2^{+} area in ML/total ML area at P12, 25.3±1.3% in WT vs. 36.0±3.0% in MMP-3$^{-/-}$ mice (n=7, p<0.05); at P15, 14.3±1.9% in WT vs. 21.2±1.8% in MMP-3$^{-/-}$ mice (n=9, p<0.05)). At P21, however, cerebella of both genotypes still contained a small but equal VGLUT2 expression in the ML. These data indicate a delay in the switch from VGLUT2 to VGLUT1, which could also be confirmed by immunostainings for VGLUT1 (data not shown). Taken together, an aberrant tangential/radial migration of differentiated GCs in the deeper EGL and an anomalous PC dendritogenesis in MMP-3$^{-/-}$ mice result in a delayed GC-PC synapse maturation.

MMP-3 Deficiency Influences Maturation of GABAergic Neurons

As MMP-3 was also expressed in all GABAergic cells and to further investigate whether the defective PC dendritogenesis and the delayed arrival of GCs in the IGL affects IN-PC synaptogenetic processes, immunostainings for VGAT, a vesicular GABA transporter, were performed. Subsequent analyses in the PCL revealed a significantly reduced number of VGAT^{+} basket cell (BC) synaptic contacts on PC soma in MMP-3$^{-/-}$ mice at P10 (n=5, p<0.01) and P12 (n=10, p<0.001). However, this was no longer visible at P15 (Fig. 4b). Also the formation of pinceaux, specialized structures of BC axon terminals on the PC axon hillock, which occur from P12 on, was transiently delayed at P12 (n=6–10, p<0.01), but normalized at P15 (n=3–4, p=NS) and in adult mice (n=9–10, p=NS) (Fig. 4b). To study whether this difference in the number of VGAT^{+} contacts is due to a reduced proliferation of BC precursors or a delayed BC migration from the WM, we stained for Pax-6, a transcriptional regulator expressed by GCs, and determined the number of Pax-6^{-}/DAPI^{+} cells as a measure for INs in the ML and PCL. These cells represent both BCs and stellate cells (SCs) coming from a common pool of GABAergic IN precursors and generated during early postnatal life [25]. Although BCs are restricted to the deeper one third of the ML, and SCs are located in the outer half [26], it is impossible to clearly distinguish both cell types. At P8, no difference in the number of INs in the ML/PCL was found, suggesting normal BC proliferation properties in MMP-3$^{-/-}$ WM during the first postnatal week. However, a significantly lower number of INs in the ML/PCL was detected in MMP-3$^{-/-}$ mice at P10 and P12, but not anymore at P15 and P21 (n≥5) (Fig. 4c). These observations implicate a transient delay in IN migration towards the ML after P8. In conclusion, our data indicate that the transiently decreased amount of VGAT^{+} synaptic contacts between the BCs and PCs in MMP-3$^{-/-}$ mice might be due to a delayed migration of INs after P8, in turn probably a secondary effect of the delayed GC arrival in the IGL.

MMP-3 Deficiency Results in Mild Motor Coordination and Balance Problems

As it is well known that an aberrant development of the cerebellar cortex can contribute to motor deficits [27], P16 MMP-3$^{-/-}$ and WT pups were subjected to treadmill gait analysis. Significantly increased mean values for front base distance (between the front paws) and left overlap distance (between overlapping left front and hind paws) (n=9, p<0.005) were recorded in MMP-3$^{-/-}$ pups (Fig. 5a), indicative for an impaired gait.

Permanent disturbances in motor performance and motor learning were further investigated in adult mice. Cage activity did not differ remarkably between the two genotypes (data not shown), suggesting that no abnormalities in activity can influence motor behavior during testing. When challenged to run an accelerating rotarod, WT mice managed to stay longer on the rotating rod as compared to their MMP-3$^{-/-}$ littermates; however, only significantly longer at the third day (n=17–14, p<0.05) (Fig. 5b). Although the interaction was not significantly different, WT animals improved their motor performance over the three consecutive days, while MMP-3$^{-/-}$ mice only enhanced their time on the rotarod significantly between day 1 and day 2. As such, this rotarod test suggests possible mild motor coordination and learning problems in MMP-3$^{-/-}$ mice. To further assess motor coordination and balance deficits, mice were forced to traverse a range of square and round beams in the balance beam test. No foot faults were noticed for both genotypes on the large square or round beam; however, by narrowing the beam, MMP-3$^{-/-}$ mice showed remarkably more difficulties traversing it (Fig. 5c). A significant interaction between genotype and beam diameter was found for performance on the round beam (p<0.0001), but significance was not

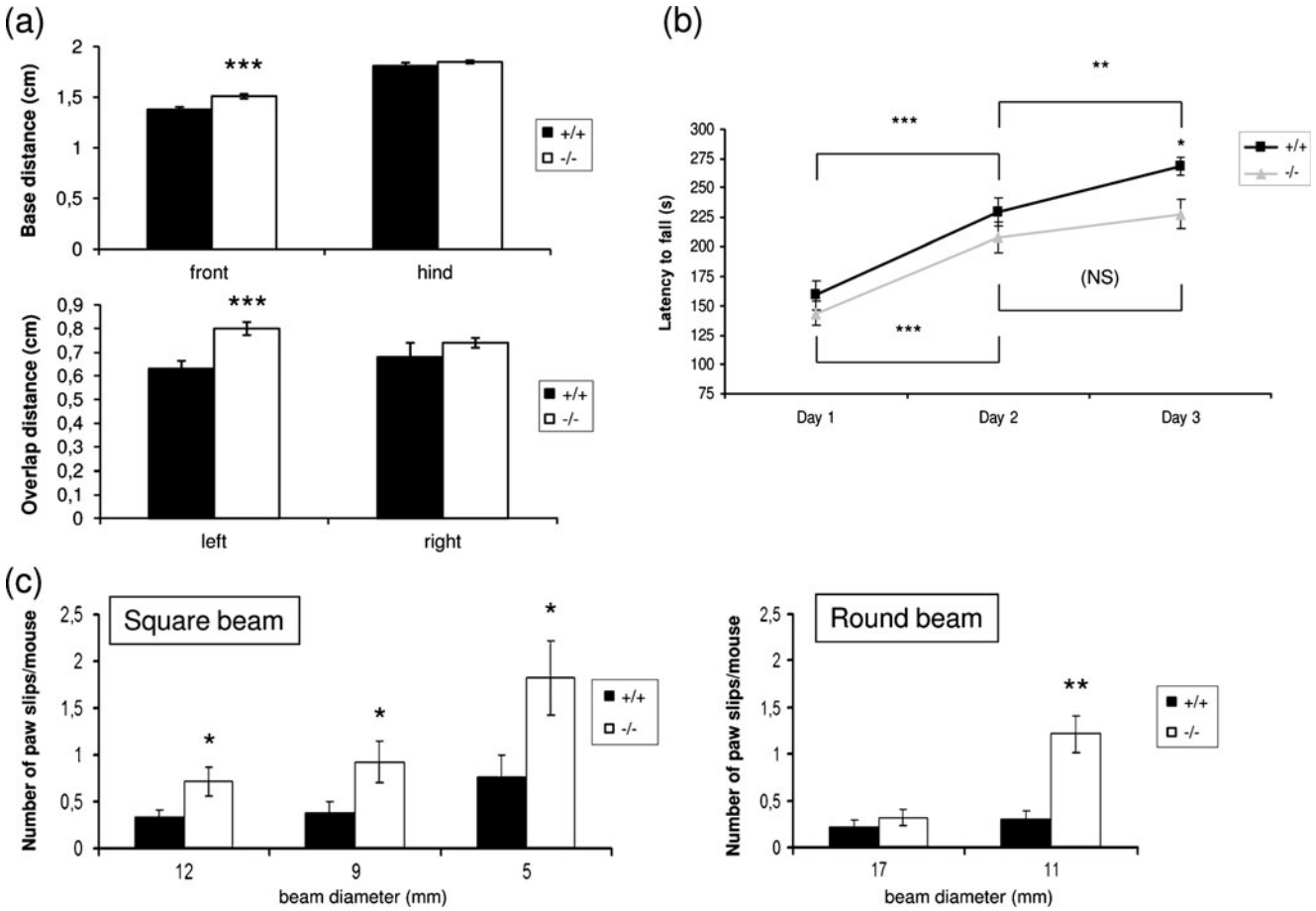

Fig. 5 Abnormal motor performance in MMP-3$^{-/-}$ animals. **a** Investigation of the gait pattern (base distance and overlap distance) of P16 pups on a treadmill shows a significantly longer front-base distance and left front-hind distance in MMP-3$^{-/-}$ mice, as compared to WT animals. **b** Adult motor performance evaluated on a rotarod reveals that MMP-3$^{-/-}$ mice spent less time on the rod; however, it is only significant on day 3. Performance of WT mice increases significantly over the three consecutive days while MMP-3$^{-/-}$ animals cannot enhance their time spent on the rotarod between day 2 and day 3. **c** WT mice also perform better in a balance beam test than their MMP-3$^{-/-}$ littermates, which make a higher number of paw slips while traversing square and round beams with decreasing diameter. As mice do not make paw slips on the largest beams (28 mm), these are not included in the graphs. Remarkably, no data could be collected for the smallest round beam as most of the MMP-3$^{-/-}$ mice fail to complete this test. Data are represented as mean±SEM (*p<0.05, **p<0.01, or ***p<0.005)

reached on the square beam. Due to frequent failures traversing the smallest round beam, we could not generate data for statistical analyses using this beam (% of failures: 11% for WT vs. 60% for MMP-3$^{-/-}$ mice, n=18–14). Finally, adult and postnatal mice were subjected to the hindlimb extension test as it is known that deviations in hindlimb extension are more often spotted in mice suffering from motor neuron anomalies [12]. However, both genotypes showed normal extension reflexes, thereby excluding possible motor neuron deficits contributing to the above described aberrant motor phenotype in MMP-3$^{-/-}$ mice (n>20).

Discussion

MMP-3 is known to play an important role in several brain pathologies [4, 28], but its involvement in brain development and neuronal wiring remains elusive. The cerebellar cortex serves as an ideal model system to study neuronal processes like proliferation, migration, and synaptogenesis. The spatiotemporal MMP-3 expression observed in the developmental rat cerebellar cortex suggests a role for MMP-3 in processes of granule cell (GC) migration and neurite outgrowth [5]. In the present study, we identified a role for MMP-3 in the development of the mouse cerebellar cortex.

Our MMP-3 mRNA and protein expression data reveal an apparent increase in expression at the beginning of the second postnatal week, suggesting a role for MMP-3 in cerebellar morphogenesis and wiring. Indeed, during this second postnatal week, GC and interneuron (IN) migration is initiated and followed by neurite extensions and synaptic wiring, concomitant with extensive Purkinje cell (PC) dendritic branching [2]. The observed MMP-3 distribution

resembles the MMP-3 expression pattern previously demonstrated in the developing rat cerebellar cortex, except for a diffuse immunopositivity around the Bergmann glia fibers in the rat ML [5], which was not present in the mouse cerebellum. Although MMPs were initially named for their ability to cleave extracellular matrix proteins, more recent evidence indicates their implication in intracellular and even intranuclear substrate cleavage. The few cellular and nuclear substrates discovered until now could associate MMP-3 with protein synthesis, transcriptional regulation, and the cytoskeleton [29]. In addition, MMP-3 is assumed to be involved in apoptosis [30–32]. However, our experiments did not reveal nuclear MMP-3 expression nor linked MMP-3 deficiency to apoptosis of cerebellar neurons during development. As MMP-3 protein expression and activity are clearly present in PC soma and primary dendrites, we hypothesize that this proteinase exerts a cell-autonomous effect on PC dendritogenesis. Despite a similar number and soma diameter of PCs in MMP-3$^{-/-}$ cerebella, a reduced PC primary dendrite length and tree size was noticed in postnatal as well as in adult MMP-3$^{-/-}$ mice. These findings correlate with an increased MMP-3 expression observed in the second postnatal week. Indeed, PC somatic growth and monolayer formation is completed at the beginning of the first postnatal week, but around P6, these PCs start extending their final primary dendrite and continue dendritic growth until P30 [2, 33].

Importantly, our study also showed an increased number of GCs in the EGL from the second postnatal week on. As proliferation, differentiation, and migration of GCs occur simultaneously with PC dendrite formation, interactions between both cell types are necessary for proper histogenesis. It is well known that PC disruption causes GC proliferation and migration deficits [34]. Indeed, PCs can affect GC proliferation and/or migration by production and release of proteins like sonic hedgehog and vascular endothelial growth factor [19, 35]. In addition, it has been suggested that PC dendrites can act as a means for regulating GC tangential migration as the GC migration route in the innermost EGL is predictably defined by the PC dendritic arbors [36]. Despite a normal GCP proliferation rate in cerebella of young MMP-3 deficient pups, immunostainings for postmitotic markers revealed a specific increase in the thickness of the deep EGL, where GCs migrate tangentially and extend their parallel fibers before inward radial migration. Together with the BrdU birthdating experiments, these findings suggest a delayed onset of GC radial migration, which consequently leads to a delayed arrival of GCs in the IGL. No major changes were detected in Bergmann glia morphology, required for an optimal GC radial migration through the ML. Ex vivo microexplant cultures, applied to mimick the process of GC tangential migration, revealed longer parallel fibers and an increased number of GCs migrated along these fibers in MMP-3$^{-/-}$ explants. Although we cannot exclude that our ex vivo observations do not entirely resemble the in vivo situation, a protracted tangential migration might contribute to the increased and sustained EGL thickness and delayed radial GC migration observed during development in MMP-3$^{-/-}$ cerebella. Thus, MMP-3 seems to affect parallel fiber outgrowth and subsequent GC tangential migration, directly or indirectly, through cleavage of signalling molecules, adhesion molecules or others present in the matrix of the microexplant. The underlying mechanisms or substrates contributing to this effect of MMP-3 remain elusive. MMP-3 might affect GC tangential migration by degrading tenascin, an MMP-3 activatable glia-derived matrix glycoprotein, known to alter parallel fiber outgrowth and thereby affecting GC migration, probably indirectly as suggested by its distribution pattern [1, 37]. On the other hand, MMP-3 might also influence GC tangential migration by modulating GC soma translocation. The chemokine stromal cell-derived factor 1α (SDF-1α) is known to prevent GCs from leaving the EGL by chemoattracting them towards the pia [38, 39]. An upregulation of MMP-3 at the correct developmental stage could degrade SDF-1α and subsequently initiate GC radial migration. Although our ex vivo data clearly indicate that MMP-3 is necessary for proper GC tangential migration, we cannot exclude any direct or indirect defects on the onset of radial migration at the EGL/ML border. One of the most prominent growth factors known to be activated by MMP-3 and contributing to cerebellar histogenesis is brain-derived neurotrophic factor (BDNF). Both pro-BDNF and BDNF show high expression in the IGL, PCL, and ML and a lower expression in the EGL, creating a concentration gradient which is necessary for proper GC migration out of the EGL. The phenotype observed in MMP-3$^{-/-}$ mice seems, in most respects, a milder version of the one described earlier in BDNF$^{-/-}$ mice [40–44]. However, Western blot analysis of pro- and mature BDNF levels were not found to be prominently altered in MMP-3$^{-/-}$ cerebella (data not shown), indicating that BDNF might not be the major MMP-3 substrate responsible for the observed cerebellar phenotype in MMP-3$^{-/-}$ mice. Other substrates out of the very broad MMP-3 degradome and known to be involved in parallel fiber outgrowth and/or GC migration are vitronectin, NMDA receptors, and MMP-9 [1, 5, 7, 38, 45–47]. Although MMP-9 shows a resembling mRNA and protein expression profile in the developing cerebellum and modulates GC exit from the EGL, MMP-9 deficiency or inhibition is known to affect GC apoptosis and reduce parallel fiber outgrowth, processes which were not affected or opposite in MMP-3$^{-/-}$ animals [5, 7].

Taken together, a deficit in MMP-3 expression can, through intracellular functioning in PCs, hamper production

of signaling cues by these latter cells and alter parallel fiber outgrowth and GC migration. However, we cannot exclude that extracellular MMP-3 functions around PC soma by (in) activating matrix proteins, receptors, signaling molecules, cell adhesion molecules, etc., or by interfering with repellent/attractive gradients of signalling molecules throughout the cerebellar cortex and as such influences GC migration and/or PC dendritogenesis. Finally, changes in input or output structures might also contribute to the observed phenotype and we cannot exclude that, e.g. defective climbing fibers in MMP-3$^{-/-}$ mice influence the Purkinje cell morphology [33].

An additional delayed GC-PC synapse maturation was found in MMP-3$^{-/-}$ cerebella as a result of the disturbed PC dendritogenesis and GC migration. As the expressed VGLUT subtype is believed to determine the efficacy of glutamatergic neurotransmission, the observed perturbations might affect cerebellar functioning [48]. In addition, a delayed basket cell–PC synapse formation was noted in MMP-3$^{-/-}$ pups from P10 on, possibly caused by a retarded GABAergic IN migration from the white matter towards the ML. Moreover, there is evidence that in the developing cerebellum, GCs influence the migration of basket and stellate cells from the white matter towards the ML [49, 50]. As such, we hypothesize that the delayed GABAergic IN migration in absence of MMP-3 is secondary to the retarded GC arrival in the IGL. Also the prolonged retention of GCs in the EGL probably accounts for the observed prolonged or increased GC proliferation at P12, as previously been suggested by in vitro and in vivo experiments for SDF-1α and observed in BDNF$^{-/-}$ mice [40, 51].

Of note, the mostly transient nature of phenotypical anomalies in the developing cerebellum and the lack of profound defects in the adult cerebellum of MMP-3$^{-/-}$ mice can be due to compensation by and/or redundancy of other MMPs. However, the observed morphological developmental defects seem to have important functional consequences. Indeed, although our behavioral data do not exclude the importance of MMP-3 in other parts of the brain involved in motor coordination and balance, they amplify the importance of MMP-3 in the developmental building up of the cerebellum. The aberrant gait pattern observed in MMP-3$^{-/-}$ pups resembles the gait abnormalities previously described in mice with defective cerebellar development [52]. In addition, impairments in motor coordination, motor learning, and balance, as demonstrated in mice with dysfunctional PCs [53], were also found in adult MMP-3$^{-/-}$ animals.

Taken together, although the exact working mechanism still needs to be determined, our findings clearly show that MMP-3 is essential to proper development of the cerebellar cortex.

Acknowledgements The authors thank Lut Noterdaeme, Ingrid Proven, Willy Van Ham, Ria Van Laer, and Julie Nys for their technical assistance, Marijke Christiaens for help with the art work, and Lut Arckens and Marc Tjwa for critical reading. This study was supported by grants from the Flemish Institute for the promotion of scientific research (IWT), the Research Council of K.U. Leuven, and the Research Foundation Flanders (FWO), all from Belgium. Inge Van Hove is a fellow of the Flemish Institute for the promotion of scientific research (IWT), Belgium.

Conflict of Interest The authors declare that they have no conflict of interest.

References

1. Hatten ME (1999) Central nervous system neuronal migration. Annu Rev Neurosci 22:511–539
2. Sotelo C (2004) Cellular and genetic regulation of the development of the cerebellar system. Prog Neurobiol 72:295–339
3. Takayama C, Inoue Y (2004) GABAergic signaling in the developing cerebellum. Anat Sci Int 79:124–136
4. Rivera S, Khrestchatisky M, Kaczmarek L, Rosenberg GA, Jaworski DM (2010) Metzincin proteases and their inhibitors: foes or friends in nervous system physiology? J Neurosci 30:15337–15357
5. Vaillant C, Didier-Bazes M, Hutter A, Belin MF, Thomasset N (1999) Spatiotemporal expression patterns of metalloproteinases and their inhibitors in the postnatal developing rat cerebellum. J Neurosci 19:4994–5004
6. Ayoub AE, Cai TQ, Kaplan RA, Luo J (2005) Developmental expression of matrix metalloproteinases 2 and 9 and their potential role in the histogenesis of the cerebellar cortex. J Comp Neurol 481:403–415
7. Vaillant C, Meissirel C, Mutin M, Belin MF, Lund LR, Thomasset N (2003) MMP-9 deficiency affects axonal outgrowth, migration, and apoptosis in the developing cerebellum. Mol Cell Neurosci 24:395–408
8. Ngimbous BB, Bourgeois F, Mas C, Simonneau M, Moalic JM (2001) Heart transplantation changes the expression of distinct gene families. Physiol Genomics 7:115–126
9. Ulrich R, Gerhauser I, Seeliger F, Baumgartner W, Alldinger S (2005) Matrix metalloproteinases and their inhibitors in the developing mouse brain and spinal cord: a reverse transcription quantitative polymerase chain reaction study. Dev Neurosci 27:408–418
10. Schefe JH, Lehmann KE, Buschmann IR, Unger T, Funke-Kaiser H (2006) Quantitative real-time RT-PCR data analysis: current concepts and the novel "gene expression's CT difference" formula. J Mol Med 84:901–910
11. Goddyn H, Leo S, Meert T, D'Hooge R (2006) Differences in behavioural test battery performance between mice with hippocampal and cerebellar lesions. Behav Brain Res 173:138–147
12. Jaworski DM, Soloway P, Caterina J, Falls WA (2006) Tissue inhibitor of metalloproteinase-2(TIMP-2)-deficient mice display motor deficits. J Neurobiol 66:82–94
13. Hager G, Dodt HU, Zieglgansberger W, Liesi P (1995) Novel forms of neuronal migration in the rat cerebellum. J Neurosci Res 40:207–219
14. Yamamoto M, Boyer AM, Crandall JE, Edwards M, Tanaka H (1986) Distribution of stage-specific neurite-associated proteins in the developing murine nervous system recognized by a monoclonal antibody. J Neurosci 6:3576–3594
15. Sherr CJ, Roberts JM (1999) CDK inhibitors: positive and negative regulators of G1-phase progression. Genes Dev 13:1501–1512
16. Kawaji K, Umeshima H, Eiraku M, Hirano T, Kengaku M (2004) Dual phases of migration of cerebellar granule cells guided by axonal and dendritic leading processes. Mol Cell Neurosci 25:228–240

17. Komuro H, Rakic P (1998) Distinct modes of neuronal migration in different domains of developing cerebellar cortex. J Neurosci 18:1478–1490
18. Lin JC, Cepko CL (1998) Granule cell raphes and parasagittal domains of Purkinje cells: complementary patterns in the developing chick cerebellum. J Neurosci 18:9342–9353
19. Wechsler-Reya RJ, Scott MP (1999) Control of neuronal precursor proliferation in the cerebellum by sonic hedgehog. Neuron 22:103–114
20. Guan CB, Xu HT, Jin M, Yuan XB, Poo MM (2007) Long-range Ca^{2+} signaling from growth cone to soma mediates reversal of neuronal migration induced by slit-2. Cell 129:385–395
21. Adcock KH, Metzger F, Kapfhammer JP (2004) Purkinje cell dendritic tree development in the absence of excitatory neurotransmission and of brain-derived neurotrophic factor in organotypic slice cultures. Neuroscience 127:137–145
22. Zhang L, Yokoi F, Jin YH, DeAndrade MP, Hashimoto K, Standaert DG, Li Y (2011) Altered dendritic morphology of Purkinje cells in Dyt1 DeltaGAG knock-in and Purkinje cell-specific Dyt1 conditional knockout mice. PLoS One 6:e18357
23. McKay BE, Turner RW (2005) Physiological and morphological development of the rat cerebellar Purkinje cell. J Physiol 567:829–850
24. Miyazaki T, Fukaya M, Shimizu H, Watanabe M (2003) Subtype switching of vesicular glutamate transporters at parallel fibre–Purkinje cell synapses in developing mouse cerebellum. Eur J Neurosci 17:2563–2572
25. Leto K, Carletti B, Williams IM, Magrassi L, Rossi F (2006) Different types of cerebellar GABAergic interneurons originate from a common pool of multipotent progenitor cells. J Neurosci 26:11682–11694
26. Fujita S (1967) Quantitative analysis of cell proliferation and differentiation in the cortex of the postnatal mouse cerebellum. J Cell Biol 32:277–287
27. Morton SM, Bastian AJ (2004) Cerebellar control of balance and locomotion. Neuroscientist 10:247–259
28. Rosenberg GA (2002) Matrix metalloproteinases in neuroinflammation. Glia 39:279–291
29. Cauwe B, Opdenakker G (2010) Intracellular substrate cleavage: a novel dimension in the biochemistry, biology and pathology of matrix metalloproteinases. Crit Rev Biochem Mol Biol 45:351–423
30. Si-Tayeb K, Monvoisin A, Mazzocco C et al. (2006) Matrix metalloproteinase 3 is present in the cell nucleus and is involved in apoptosis. Am J Pathol 169:1390–1401
31. Wetzel M, Li L, Harms KM, Roitbak T, Ventura PB, Rosenberg GA, Khokha R, Cunningham LA (2008) Tissue inhibitor of metalloproteinases-3 facilitates Fas-mediated neuronal cell death following mild ischemia. Cell Death Differ 15:143–151
32. Choi DH, Kim EM, Son HJ, Joh TH, Kim YS, Kim D, Flint Beal M, Hwang O (2008) A novel intracellular role of matrix metalloproteinase-3 during apoptosis of dopaminergic cells. J Neurochem 106:405–415
33. Tanaka M (2009) Dendrite formation of cerebellar Purkinje cells. Neurochem Res 34:2078–2088
34. Feddersen RM, Ehlenfeldt R, Yunis WS, Clark HB, Orr HT (1992) Disrupted cerebellar cortical development and progressive degeneration of Purkinje cells in SV40 T antigen transgenic mice. Neuron 9:955–966
35. Ruiz de Almodovar C, Coulon C, Salin PA, Knevels E, Chounlamountri N, Poesen K, Hermans K, Lambrechts D, Van Geyte K, Dhondt J, Dresselaers T, Renaud J, Aragones J, Zacchigna S, Geudens I, Gall D, Stroobants S, Mutin M, Dassonville K, Storkebaum E, Jordan BF, Eriksson U, Moons L, D'Hooge R, Haigh JJ, Belin MF, Schiffmann S, Van Hecke P, Gallez B, Vinckier S, Chedotal A, Honnorat J, Thomasset N, Carmeliet P, Meissirel C (2010) Matrix-binding vascular endothelial growth factor (VEGF) isoforms guide granule cell migration in the cerebellum via VEGF receptor Flk1. J Neurosci 30:15052–15066
36. Liesi P, Akinshola E, Matsuba K, Lange K, Morest K (2003) Cellular migration in the postnatal rat cerebellar cortex: confocal-infrared microscopy and the rapid Golgi method. J Neurosci Res 72:290–302
37. Imai K, Kusakabe M, Sakakura T, Nakanishi I, Okada Y (1994) Susceptibility of tenascin to degradation by matrix metalloproteinases and serine proteinases. FEBS Lett 352:216–218
38. Komuro H, Yacubova E (2003) Recent advances in cerebellar granule cell migration. Cell Mol Life Sci 60:1084–1098
39. McQuibban GA, Butler GS, Gong JH, Bendall L, Power C, Clark-Lewis I, Overall CM (2001) Matrix metalloproteinase activity inactivates the CXC chemokine stromal cell-derived factor-1. J Biol Chem 276:43503–43508
40. Borghesani PR, Peyrin JM, Klein R, Rubin J, Carter AR, Schwartz PM, Luster A, Corfas G, Segal RA (2002) BDNF stimulates migration of cerebellar granule cells. Development 129:1435–1442
41. Hisatsune C, Kuroda Y, Akagi T, Torashima T, Hirai H, Hashikawa T, Inoue T, Mikoshiba K (2006) Inositol 1,4,5-trisphosphate receptor type 1 in granule cells, not in Purkinje cells, regulates the dendritic morphology of Purkinje cells through brain-derived neurotrophic factor production. J Neurosci 26:10916–10924
42. Lee R, Kermani P, Teng KK, Hempstead BL (2001) Regulation of cell survival by secreted proneurotrophins. Science 294:1945–1948
43. Schwartz PM, Borghesani PR, Levy RL, Pomeroy SL, Segal RA (1997) Abnormal cerebellar development and foliation in $BDNF^{-/-}$ mice reveals a role for neurotrophins in CNS patterning. Neuron 19:269–281
44. Xu ZQ, Sun Y, Li HY, Lim Y, Zhong JH, Zhou XF (2011) Endogenous proBDNF is a negative regulator of migration of cerebellar granule cells in neonatal mice. Eur J Neurosci 33:1376–1384
45. Hahn-Dantona E, Ramos-DeSimone N, Sipley J, Nagase H, French DL, Quigley JP (1999) Activation of proMMP-9 by a plasmin/MMP-3 cascade in a tumor cell model regulation by tissue inhibitors of metalloproteinases. Ann N Y Acad Sci 878:372–387
46. Imai K, Shikata H, Okada Y (1995) Degradation of vitronectin by matrix metalloproteinases-1, -2, -3, -7 and -9. FEBS Lett 369:249–251
47. Pauly T, Ratliff M, Pietrowski E, Neugebauer R, Schlicksupp A, Kirsch J, Kuhse J (2008) Activity-dependent shedding of the NMDA receptor glycine binding site by matrix metalloproteinase 3: a PUTATIVE mechanism of postsynaptic plasticity. PLoS One 3:e2681
48. Takamori S (2006) VGLUTs: 'exciting' times for glutamatergic research? Neurosci Res 55:343–351
49. Guijarro P, Simo S, Pascual M, Abasolo I, Del Rio JA, Soriano E (2006) Netrin1 exerts a chemorepulsive effect on migrating cerebellar interneurons in a Dcc-independent way. Mol Cell Neurosci 33:389–400
50. Leto K, Bartolini A, Rossi F (2008) Development of cerebellar GABAergic interneurons: origin and shaping of the "minibrain" local connections. Cerebellum 7:523–529
51. Klein RS, Rubin JB, Gibson HD, DeHaan EN, Alvarez-Hernandez X, Segal RA, Luster AD (2001) SDF-1 alpha induces chemotaxis and enhances sonic hedgehog-induced proliferation of cerebellar granule cells. Development 128:1971–1981
52. Meng H, Larson SK, Gao R, Qiao X (2007) BDNF transgene improves ataxic and motor behaviors in stargazer mice. Brain Res 1160:47–57
53. Sausbier M, Hu H, Arntz C, Feil S, Kamm S, Adelsberger H, Sausbier U, Sailer CA, Feil R, Hofmann F, Korth M, Shipston MJ, Knaus HG, Wolfer DP, Pedroarena CM, Storm JF, Ruth P (2004) Cerebellar ataxia and Purkinje cell dysfunction caused by Ca2+-activated K+ channel deficiency. Proc Natl Acad Sci USA 101:9474–9478